Monte Carlo Calculations of Order Parameter Profiles in Models of Lipid–Protein Interactions in Bilayers†

H. L. Scott
Department of Physics, Oklahoma State University, Stillwater, Oklahoma 74078
Received February 13, 1986; Revised Manuscript Received May 23, 1986

ABSTRACT: The Monte Carlo method has been utilized to calculate lipid chain order parameters in model monomolecular layers (half-bilayers) containing several different model polypeptides. The systems all consist of a periodic array of identical cells, each containing 35 hydrocarbon chains and 1 "perturbant" (a small model polypeptide or protein). The lipid chains are each 10 CH_2 subunits long, have one end constrained to lie in the bilayer plane, and interact via van der Waals forces between all subunits. The chains also interact with the perturbant via van der Waals forces. With standard Monte Carlo procedures order parameter profiles are calculated for chains that are close to the perturbant and for the nonneighboring chains. In order to examine a wide range of possibilities, several different model polypeptides are considered: (i) a rigid smooth cylinder, (ii) a cylinder with identical side chains at α-helical positions, (iii) a cylinder with nonidentical side chains at α-helical positions, and (iv) a cylinder identical with (ii) but which only extends about halfway through the monolayer. Although results differ for the different systems studied, in all cases only slight conformational differences between the bulk chains and the chains that are nearest the perturbants are found, and it is not possible to characterize the boundary chains as "more ordered" or "less ordered" than the nonboundary chains.

The detailed manner in which the presence of proteins in lipid bilayers affects the behavior of the lipids themselves has been under intensive study for almost two decades. Due to the diversity of membrane proteins and lipids and in large part to difficulties encountered in performing the experiments and in interpreting the data, many questions remain controversial. A major point of interest concerns the nature of boundary lipid, i.e., the lipid chains in direct contact with the hydrophobic core of the membrane protein. Early ESR studies (Jost et al., 1973; Jost & Griffiths, 1980) indicated that the lipid within an annular region around a protein was ordered differently than the bulk lipid on the ESR time scale while NMR studies (Rice et al., 1979a,b; Paddy et al., 1981; Bienvenue et al., 1982; Deveaux & Seigneuret, 1985) indicate that on much longer time scale the distinction between two types of lipid disappears. Differential scanning calorimetry experiments (Papahadjopoulos et al., 1975; Gomez-Fernandez et al., 1980; Hapman et al., 1977) show that the presence of integral proteins in bilayers reduces the cooperativity of the lipid chain melting phase transition, and a common conclusion is that a number of lipid molecules are removed or somehow isolated from the bulk lipid by each protein in the bilayer [for example Rigell (1985)]. Very recent NMR and scanning calorimetry studies of model polypeptide–lipid bilayers indicate that the situation may be even more complex, involving phase separations hitherto overlooked (Huschilt et al., 1985; Morrow et al., 1985). Energy-transfer studies of bacteriorhodopsin model membranes have been interpreted as revealing very long-range (45 Å or more) interactions between protein molecules (Rehorek et al., 1985).

A number of differential theoretical investigations of lipid–protein interactions have been carried out in recent years. Early studies were based upon the assumption that lipid chains nearest to protein molecules are forced into more ordered conformations (Marcelja, 1976; Owicki et al., 1978; Owicki, 1980; Jahnig, 1981; Scott & Coe, 1984). The mean field model of Marcelja (1976) and the Euler–Lagrange calculations of Owicki et al. (1978, 1980) predicted monotonically decaying molecular order as the distance from an integral protein increased, but such a structure in equilibrium (i.e., long time scales) is not supported by NMR measurements. Phase-transition models using purely hard-core interactions (Scott & Coe, 1984) predicted transition temperatures that decreased too rapidly with protein concentration, and attempts to rectify the disagreement by allowing each protein to partially "swallow" some lipid molecules (Scott & Coe, 1984) did not fit the data well unless the number of swallowed molecules was allowed to become quite large. In summarizing these theoretical efforts, one could say that models using simple lipid–protein interactions or idealized approximations are not yet able to accurately describe all aspects of lipid–protein mixtures. The recently published "mattress model" (Mouritsen & Bloom, 1985) is an attempt to consider more complex interactions and hydrophobic mismatches. However, without a clear picture of lipid–protein energetics at the molecular level, it is very hard to decide which types of interactions should be included in any model, and even harder to accurately analyze the models mathematically.

In this paper the results of an extensive series of calculations aimed at improving the molecular picture of lipid–protein interactions are presented. The calculations make use of the Monte Carlo method for deriving equilibrium properties of many-body systems. The advantages gained in using a computer to simulate the systems are that one can work with much more realistic models and forces than analytic theoretical efforts allow, and localized properties of the systems may be studied. The major disadvantages are of course that one must work with very small numbers of molecules and that true equilibration in complex systems may be difficult to attain. In the past several years there have been a number of computer studies of lipid bilayers. Two general types of simulations that

† This work supported in part by the U.S. Department of the Interior as authorized by the Water Research Development Act of 1979. Contents of this publication do not necessarily reflect the views and policies of the U.S. Department of the Interior.

0006-2960/86/0425-6122$01.50/0 © 1986 American Chemical Society

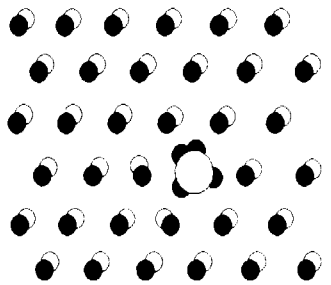

FIGURE 1: Schematic diagram of a typical simulation cell with lipid chains in an hexagonal array (the initial state) and a model polypeptide. The interchain separation is 5.7 Å. Because the interchain van der Waals radius is 3.9 Å, the chains fill more of the space than the figure suggests. The semicircles in the polypeptide represent projections of four side chains each rotated 110° and vertically displaced 1.5 Å from its predecessor.

have appeared are (i) Monte Carlo calculations of the properties of lattice models for lipid bilayers [for a review see Mouritsen (1984)] and (ii) Monte Carlo and molecular dynamics studies of continuum models of bilayers containing flexible chains interacting via realistic potentials (Scott, 1977; Scott & Cherng, 1978, Kox et al., 1980; van der Ploeg & Berendsen, 1983). With the exception of studies of highly simplified lattice models (Pink et al., 1982), all of the numerical work has been done for pure lipid systems, and no detailed numerical analysis of the lipid–protein interface has been performed before. The work reported in this paper was carried out because computer calculations offer a unique opportunity to view lipid–protein interactions at a fundamental level, which can be an aid in experimental interpretation as well as theoretical model building. In the next section a detailed description of the models and the numerical methods used are given. In the third section the results will be presented. The final section is a discussion of these results and of the limitations of the methodology.

Methods and Models

The Monte Carlo approach used is similar to that used earlier by the Scott (1977), with improvements in the treatment of the rotational motions and the interactions between molecules. Four different types of lipid–polypeptide interactions were modeled, and each will be described in turn. In common to all systems is an array of 35 single-chain molecules, each 10 CH_2 subunits in length. The chains are allowed to translate laterally in a plane to which the top CH_2 is anchored. Near the top CH_2 the chains are oriented perpendicular to the plane of translation but may change conformation via gauche rotations about any of the bonds. In the lipid array there is a single polypeptide molecule. Figure 1 shows a top view of a typical array in which the chains are all perpendicular to the plane. The larger object is the polypeptide, which is held immobile in these studies. The energy of a chain is a sum of its internal energy due to gauche rotations and the van der Waals interaction energy of all the subunits with all other chain and peptide subunits within the interaction range

$$E_{\text{chain}} = \sum_{\text{bonds},i} E(i) + \sum_{\text{CH}_2\text{'s } i \neq j} \sum \epsilon[(\sigma/r_{ij})^{12} - (\sigma/r_{ij})^{6}] \quad (1)$$

where $E(i)$ is 500 cal/mol for a gauche bond surrounded by trans bonds and is 2500 cal/mol for successive gauche bonds. The parameters σ and ϵ are the van der Waals radius and energy, respectively (to be discussed below), and r_{ij} is the distance between two methylenes on chains i and j. The rotational isomer model is used so that the only allowed gauche rotations are ±120°. Recently several authors have used larger gauche energies than 500 cal/mol (Bartell & Kohl, 1963; Nagle, 1986). In this work the results are not sensitive to changes of ±100 cal/mol in $E(i)$. The values chosen for the van der Waals parameters are

$$\sigma = 3.905 \text{ Å} \qquad \epsilon = 118 \text{ cal/mol} \quad (2)$$

from the optimizing potential studies of Jorgensen et al. (1984). As will be discussed in more detail later, the most important factor is the van der Waals radius σ. Four different types of model polypeptides were considered.

Model 1: A rigid cylinder of van der Waals radius 4.5 Å interacting with the chains via a cylindrically symmetric 6–12 potential with σ = 4.5 Å and ϵ given by eq 2. The dimensions of the planar cell are 29.1 × 34.2 Å^2 with periodic boundary conditions imposed.

Model 2: A rigid cylinder of radius 2.0 Å with seven identical spherical side chains of van der Waals radius 3.9 Å protruding at α-helical positions. The side chains were treated identically as the chain subunits for the purpose of energy calculations. Since this model polypeptide has greater lateral area, the planar cell dimensions are 30 × 36 Å^2 with periodic boundary conditions imposed.

Model 3: A rigid cylinder identical with model 2 except the van der Waals radii of the side chains take on the values 5, 4.5, and 3.9 Å successively along the cylindrical core. The energy parameter ϵ is still 118 cal/mol.

Model 4: A rigid cylinder identical with model 2 except that it extends only halfway through the monolayer.

In all cases the dimensions of the cell are adjusted to produce an area per chain of about 29 Å^2 (after subtracting out the approximate area of the perturbant). This area is roughly equivalent to the lipid bilayer area per chain in the fluid phase. The nonsymmetric shape of the cell area is designed to initialize the chains in an hexagonal array (Figure 1). A typical Monte Carlo runs proceeds by stepping through the system of chains sequentially. At each step the chain in question is translated in the layer plane by a random distance less than 0.15 Å. With probability $^1/_2$, gauche rotations may then be attempted (it was found that attempting gauche rotations at every step led to extremely high rejection rates at the chain densities considered here). When gauche rotations are attempted the procedure is to pick one or two nonconsecutive bonds at random. If one bond is picked, its gauche state is changed from the state prior to the move to another of the three possible isomeric states accessible to each bond. If two bonds are considered, the higher bond is changed as described and the lower bond is changed in the opposite direction. For a chain that is initially in all-trans conformation this sequence favors kink and jog formation. After many passes, however, all accessible conformations are possible. The major differences between the present Monte Carlo algorithm and the procedure employed earlier by Scott (1977) are that multiple rotations are considered in a fraction of the moves, and no rotations at all are attempted in a fraction of the moves. It was found by trial and error that the rejection rate is reduced to about 60%, and convergence rates are faster when these changes are incorporated. Further, at realistic chain densities it is important to attempt some multiple-bond conformational changes to avoid many rejections due to steric hindrances. After the new state (position, conformation) is chosen, the new van der Waals and isomeric energies are calculated. The interaction energy calculation is the part of the program requiring the most time. In order to save computer time a finite interaction range of 10 Å is used to construct a neighbor matrix (so that all intersubunit distances need not be recomputed at every step). Two chains are defined to be neighbors if any

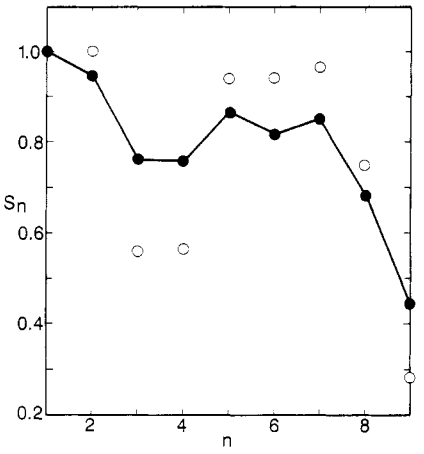

FIGURE 2: Order parameter profiles for model 1. The open circles are data points for nearest-neighbor chains, while the solid line connects points calculated for bulk chains.

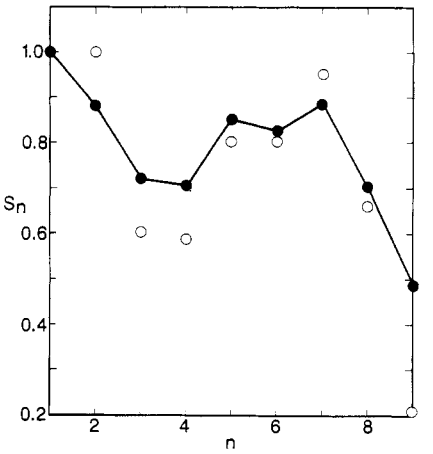

FIGURE 3: Order parameter profiles for model 2. The open circles are data points for nearest-neighbor chains, while the solid line connects points calculated for bulk chains.

subunit of one chain is within the interaction range of any subunit of the other chain. Then the potential energy, Eq 1, is calculated only for pairs of chains defined as neighbors. The neighbor matrix is updated every 10 passes through the system. The total energy of a chain therefore consists of its intramolecular energy due to isomerism and its energy of interaction with its neighbors.

Comparing the new chain energy with its energy in the previous configuration, the move is accepted or rejected according to standard Monte Carlo sampling procedures (Metropolis et al., 1950) at 300 K. After each step the order parameters

$$S_n = \tfrac{1}{2}[3\cos^2(\theta_n - 1)] \quad (3)$$

are calculated, where θ_n is the angular deviation of bond n from its orientation with respect to the chain axis in the all-trans state. Three such averages are computed: order parameters for the chains that are nearest the perturbant (using the criteria that one subunit must be within 8 Å of the perturbant for a chain to be considered a neighbor); "bulk" chains (those chains that are not neighbors to the perturbant); all chains regardless of location in the plane.

All computations were performed on the Oklahoma State University IBM 3081K mainframe machine using the pseudorandom number program RANF and starting at different points in the random-number sequence for each run. Typically, a calculation started from a lattice as shown in Figure 1 and was equilibrated for 350000 configurations. Averages were then calculated over a further 490000 configurations. Checks on convergence were performed by restarting a system from the lattice at a different point in the random-number sequence and comparing final results, or, in one case, by carrying out an extremely long run of 800000 configurations. The estimated errors in the results depend upon the bond number n. For n = 2–3 (n = 1 is the bond closest to the interface plane and does not deviate from the trans orientation) error is estimated to be 5%. For n = 4–6 the estimated error is 10%. For n = 7–9 the estimated error is 15%.

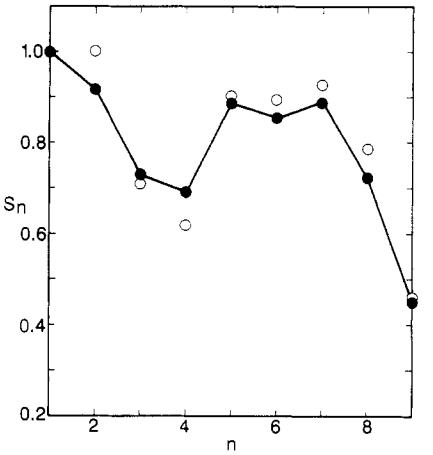

FIGURE 4: Order parameter profiles for model 3. The open circles are data points for nearest-neighbor chains, while the solid line connects points calculated for bulk chains.

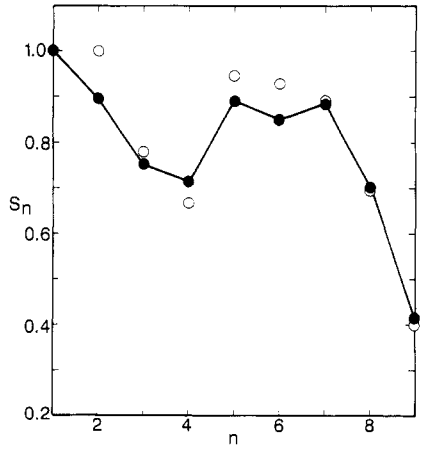

FIGURE 5: Order parameter profiles for model 4. The open circles are data points for nearest-neighbor chains, while the solid line connects points calculated for bulk chains.

Results and Discussion

Figures 2–5 show the resulting order parameter profiles calculated for each of the four models. Each figure contains a plot of the profile for the nearest-neighbor chains relative to the polypeptide and the profile for the entire sample of chains. Close examination of the bulk chain profiles in each figure shows that they are nearly identical, and this is a good indication that the model systems were all in equilibrium during the profile calculations. As was the case in earlier Monte Carlo studies of hard-sphere chains (Scott, 1977) the order parameters do not reflect chain tilting and are therefore uniformly larger than the values obtained by NMR measurements. As a first approximation one argues that the tilting provides, approximately, an overall multiplicative scale factor of about 0.5–0.6 (Petersen & Chan, 1977) to the data. The

presence of the model polypeptide may also affect chain tilting, but this should be minimal for the models studied here because no hydrophobic mismatches are considered. In the case of membrane proteins, which are though to consist in many cases of several helical subunits, the protein is much larger than can be studied by our method, but in this case chains will interact with a large polypeptide interface regardless of their tilt angle. It therefore is likely that the results presented here will not be strongly affected by chain-tilt considerations.

The bulk lipid profiles in Figures 2–5 differ from those of our earlier simulations (Scott, 1977) in the following ways: First, from the first rotatable bond to the end of the chain all S_n are smaller than the earlier data. Second, there is a dip in the profiles and the n = 3–4 positions that is not present in the earlier calculations. The uniformly smaller values of the S_n show that the present algorithm more effectively samples the space of accessible conformations that the earlier version (indeed rejection rates for these calculations are substantially less than those of the earlier runs at comparable densities). The dip in the data is also seen (to a lesser extent) in experimental studies of sodium decanoate (Seelig & Niederberger, 1974) and dipalmitoylphosphatidylcholine (Schindler & Seelig, 1975) (recall from above that the data in Figures 2–5 should be scaled by a factor of 0.5–0.6 due to tilting before comparing with experimental work). The dip in the experimental data occurs at the same place as that in the simulations if the first bond that can reorient is labeled 1 instead of 2. Equivalently, one could present the data in terms of the order of the CH_2 groups starting with the first movable one at the end of bond no. 1. Order parameters for the CH_2's are defined in terms of the deviation of the CH_2 plane from the parallel to the bilayer plane, and the results are identical with those displayed for the bonds. In either case the dip in the data occurs at the *same* location as the experimental dip. This feature of the data may be a result of the fact that a gauche bond inserted in a position near the top of a chain is not likely to be as easy to remove as one closer to the bilayer center. Thus, such bonds may have slightly longer lifetimes than average. The fact that the dip in the profiles in Figures 2–5 is larger than experiment is then a result of the inability of the algorithm to sample all possible types of chain motions as efficiently or as quickly as the chains themselves do. The presence of the dip in the S_n vs. n profiles in Figures 2–5 suggests that the present simulations are a considerable improvement over the previous work.

Figure 2 gives the results of the studies of model 1, in which the polypeptide was modeled as a rigid cylinder of van der Waals radius 4.5 Å, roughly the hard-core size of an α helix without side chains. Somewhat surprisingly, the greatest difference between the nearest-neighbor profile and the total system profile occurs for this model. The smooth appendage-free surface apparently induces more of the neighboring chains to form kinks or jogs in the n = 3–4 region. This accounts for the lowered values of the order parameters for n = 3–4 and the larger values for n = 5–7. The dip at the n = 3–4 positions is greater for the nearest-neighbor chains in this model than for any of the other models. A possible explanation is that the smooth surface leaves less free volume for all the neighboring chains, so that once inserted, gauche bonds at n = 3–4 are harder to remove than in the bulk system. By contrast, in models 2–4 the model peptides have asymmetrical bulges (the side chains), and not all of the neighboring chains are near a bulge, which restricts motions near the chain tops.

Figure 3 gives the results of the studies of model 2, in which side chains of van der Waals radius 3.9 Å are added to a 2-Å radius cylinder, producing a lumpier surface with maximum radius 5.9 Å. In this case the conformations found for chains close to the helix are almost the same as those for model 1, indicating that the side chains in this model do not significantly alter the set of allowed conformations of the lipid chains. One difference is that the n = 3–4 dip is not quite as pronounced as that of model 1, although the error bars for the two models for these points overlap. Figure 4 gives the results of studies of model 3, in which additional roughness was added to model 2 by assigning side chains different van der Waals radii. There are obviously many ways such assignments may be made, and no attempt was made to consider all possibilities. The results reported here are for a system in which the seven side chains were given radii 3.9, 4.5, 3.9, 5.0, 3.9, 4.5, and 3.9 Å (respectively from the chain closest to the interface plane downward). Examination of Figure 4 shows that the asymmetry produced slightly greater disordering at the n = 3–4 positions and slightly less disordering at the n = 8–9 ends. This specific profile must be related to the particular pattern chosen for the locations of the different sized side chains. In particular the chain with radius 5.0 Å should have the greatest effect on the order parameters in the boundary region. In model 3 this chain sits roughly in the middle of the layer.

Model 4 represents an attempt to construct a system for which a greater difference between the boundary chains and the bulk chains might be observed by terminating the helix of model 2 after the second side chain (which has center 2.5 Å below the interfacial plane and radius 3.9 Å). It was felt that this would give neighbor chains a region of free volume to fold into, resulting in lower order parameters for the bottom two to three bonds than is possible in the bulk. As Figure 5 shows, the effort did not prove successful in that the order at the n = 3–4 positions was not significantly lowered over the values exhibited by the other models. In retrospect, this is not surprising. The model peptide extends, on average, halfway across the chain monolayer *as measured when the chains are perfectly straight*. With two to three gauche bonds per chain, the average chain length is reduced to the point where the difference between the position of the chain terminii and the bottom of the model peptide (including the full extent of the lowest side chain) is insufficient to allow the chains to fold into the free volume. Study of a system in which the peptide only penetrates, e.g., 25% of the monolayer thickness would likely produce the desired results. It is clear from the earlier studies (Scott, 1977; Scott & Cherng, 1978) that free volume is a major factor in the determination of order parameter profiles.

Conclusions

The main conclusion to be drawn from the calculations reported here is that a single polypeptide chain aligned perpendicular to the bilayer plane does not greatly perturb the equilibrium lipid chain states as measured by the order parameter profiles. A persistent lowering of the order parameters at n = 3–4 is seen in the boundary chains, compared to the bulk chains, but average order parameters over all bonds are nearly identical for boundary and bulk lipid. These conclusions apply to all the models studied, so that details of side-chain location and size have little effect on the differences in the equilibrium average lipid chain conformations between chains near the peptide and bulk chains. Two important types of motions are not included in the calculations: peptide side-chain motions and lipid lateral motions that involve chains diffusing over distances large compared to a chain diameter. The former motions were not included to avoid the extra computational effort required, and the latter motions simply do not occur

during the duration of any of the simulations (this is because multiple-chain cooperative translations are not considered, and within the Monte Carlo method used here, a change in any single-chain configuration represents an entirely new system configuration that could equivalently be attained by some suitable lateral diffusive motion). The most likely effect of the two neglected degrees of freedom should be to further reduce the difference between boundary and bulk chains.

Of course the calculations reported here are for *model* systems. Besides the two motional degrees of freedom mentioned above, the models do not consider the nonspherical shapes of the CH_2 subunits or the peptide side chains, the motion of the polypeptide as a whole, or chain displacements perpendicular to the bilayer plane. However, the calculations reported above, as well as earlier work (Scott, 1977; Kox et al., 1978), strongly support the idea that the most crucial factor affecting chain conformations is the excluded volume effect, and this is certainly included in these simulations. The neglected factors should, in my estimation, act to reduce slightly and distinction between boundary and bulk chain conformations. The major conclusion of this work is, then, that a single α helix, even with fairly large side chains, perturbs equilibrium lipid chain conformational order only slightly in the midchain positions and this perturbation is the nearly the same as would be caused by a smooth rod of appropriate radius.

If there is little difference between bulk and boundary chains, at least over thermal equilibrium time scales, and if there are no strong electrostatic or hydrogen-bonding interactions between lipid and protein, then there is no "lipid-mediated" interprotein force (Marcelja, 1976), and protein aggregation must be consequence of direct (for example electrostatic) interprotein interactions or a consequence of protein preference for certain lipid phases. Proteins will affect the lipid phases in bilayers even without strong local interactions by disrupting the cooperativity of the system near the transition temperatures. This, plus a preference by the protein for, e.g., the fluid bilayer phase, can lead to domain formation and phase separation such as recently reported in lipid–protein mixtures (Huschilt et al., 1985; Morrow et al., 1985).

References

Bartell, L. S., & Kohl, D. A. (1963) *J. Chem. Phys. 39*, 1114–1123.

Bienvenue, A., Bloom, M., Davis, J. H., & Deveaux, P. F. (1982) *J. Biol. Chem. 257*, 3032–3038.

Chapman, D., Gomez-Fernandez, J. C., & Goni, F. M. (1979) *FEBS Lett. 98*, 211–223.

Deveaux, P., & Siegneuret, M. (1985) *Biochim. Biophys. Acta 822*, 63–125.

Gomez-Fernandez, J. C., Goni, F. M., Bach, D., Restal, A. J., & Chapman, D. (1980) *Biochim. Biophys. Acta 598*, 502–516.

Huschilt, J. C., Hodges, R. S., & Davis, J. H. (1985) *Biochemistry 24*, 1377–1386.

Jahnig, F. (1981) *Biophys. J. 36*, 329–345.

Jorgensen, W. L., Madura, J. D., & Swenson, C. J. (1984) *J. Am. Chem. Soc. 106*, 6638–6696.

Jost, P. C., & Griffith, O. H. (1980) *Ann. N.Y. Acad. Sci.* 391–405.

Jost, P., Griffith, O. H., Capaldi, R. A., & Vanderkooi, G. (1973) *Proc. Natl. Acad. Sci. U.S.A. 70*, 480–484.

Kox, A. J., Michels, J. P. J., & Weigel, F. W. (1978) *Nature (London) 287*, 317–319.

Marcelja, S. (1976) *Biochim. Biophys. Acta 455*, 1–7.

Metropolis, N., Rosenbluth, A., Rosenbluth, M., Teller, A., & Teller, E. (1953) *J. Chem. Phys. 21*, 1087–1096.

Morrow, M. R., Huschilt, J. C., & Davis, J. H. (1985) *Biochemistry 24*, 5396–5406.

Mouritsen, O. (1984) *Computer Studies of Phase Transitions and Critical Phenomena*, Springer-Verlag, New York.

Mouritsen, O. G., & Bloom, M. (1984) *Biophys. J. 46*, 141–153.

Nagle, J. F. (1986) *Faraday Soc. Disc.* (in press).

Owicki, J. C. (1981) *Comments Cell. Mol. Biophys. 1*, 83–92.

Owicki, J. C., Springate, M. W., & McConnell, H. M. (1978) *Proc. Natl. Acad. Sci. U.S.A. 75*, 1616–1619.

Paddy, M. R., Dahlquist, F. W., Davis, J. H., & Bloom, M. (1981) *Biochemistry 20*, 3152–3162.

Papahadjopoulos, D., Moscarello, M., Eylar, E. H., & Isac, T. (1975) *Biochim. Biophys. Acta 401*, 317–355.

Petersen, N. O., & Chan, S. I. (1977) *Biochemistry 16*, 2657–2667.

Pink, D. A., Georallas, A., & Chapman, D. (1981) *Biochemistry 20*, 7152–7157.

Rehorek, M., Dencher, N. A., & Heyn, M. P. (1985) *Biochemistry 24*, 5980–5988.

Rice, D. M., Hsung, J. C., King, T. E., & Oldfield, E. (1979) *Biochemistry 18*, 5885–5892.

Rigell, C. W., de Saussure, C., & Freire, E. (1985) *Biochemistry 24*, 5638–5646.

Schindler, H., & Seelig, J. (1975) *Biochemistry 14*, 2283–2287.

Scott, H. L. (1977) *Biochim. Biophys. Acta 469*, 264–271.

Scott, H. L., & Cherng, S.-L. (1978) *Biochim. Biophys. Acta 510*, 209–215.

Scott, H. L., & Coe, T. J. (1984) *Biophys. J. 42*, 219–228.

Seelig, J., & Niederberger, W. (1974) *Biochemistry 13*, 1585–1588.

van der Ploeg, P., & Berendsen, H. J. C. (1983) *Mol. Phys. 49*, 233–256.